Theor Chem Acc (2012) 131:1212
DOI 10.1007/s00214-012-1212-0

REGULAR ARTICLE

Wave-packet propagation study of the early-time non-adiabatic dissociation dynamics of NH_3Cl: Diabatic picture, effects of isotope substitution and varying the initial vibration levels

Young Choon Park · Heesun An · Heechol Choi · Yoon Sup Lee · Kyoung Koo Baeck

Received: 16 February 2012 / Accepted: 21 March 2012 / Published online: 4 April 2012
© Springer-Verlag 2012

Abstract Reduced two-dimensional (2D) diabatic potential energy surfaces (PESs) of the two lowest electronic states of NH_3Cl were constructed by using the adiabatic 2D PESs, and the early-time dissociation dynamics of the charge-transferred excited electronic state of NH_3Cl (Ronen et al. in Phys Rev Lett 93:048301, 2004) were investigated. In the diabatic representation, it was shown that the dissociation path from H_2NH^+–Cl^- to $H_2N + HCl$ includes two different processes: the one-step dynamics of diabatic proton transfer followed by electron adjustment, and the two-step dynamics consisting of firstly electron transfer from the other direction mediated (stimulated) by proton movement to form the ground electronic state of H_2NH–Cl and then secondly adiabatic H atom tunneling to H_2N–HCl. In order to find a means of controlling the branching ratio of the two paths toward the $H_2N + HCl$ and $H_2NH + Cl$ limits, the effects of varying the initial vibration levels of the precursor anion NH_3Cl^- and those of isotope substitution (H_2NDCl) were also studied. Only the $H_2N + HCl$ limit was observed regardless of the initial vibration level and isotope substitution. The overall features of the dynamics are almost unchanged by deuterium substitution (H_2NDCl); only the timescale is increased, as expected.

Y. C. Park · H. Choi · Y. S. Lee (✉)
Department of Chemistry, Korea Advanced Institute of Science and Technology (KAIST), Daejeon 305-701, Republic of Korea
e-mail: yslee@kaist.edu

H. An · K. K. Baeck (✉)
Department of Chemistry, Gangneung-Wonju National University, Gangneung 210-702, Republic of Korea
e-mail: baeck@gwnu.ac.kr

Keywords NH_3Cl · Dissociation dynamics · Wave-packet propagation · Non-adiabatic · Diabatic picture · Effects of initial vibration levels

1 Introduction

Proton transfer via an excited charge-transfer state has been widely investigated during recent decades [1] because of its important role in many chemical and biological systems. The ammonia halogen complex (NH_3Cl) is one of the simplest cases of a proton and charge–transfer molecule. Cheshnovsky and coworkers [2, 3] originated the study of the charge-transfer state of neutral NH_3Cl. They reported experimental results showing that neutral NH_3Cl dissociates through the charge-transfer excited state, H_2NH^+–Cl^-, which is generated by the electron photo-detachment of its anion, NH_3Cl^-. This process can be considered as one of the simplest proton-coupled electron-transfer (PCET) phenomena, yet the transfers of the electron and the proton occur in different directions, which is sometimes called bidirectional PCET [1]. The basic features of the experimental results were explained with the theoretical results of Kaldor [4]; he obtained stationary geometries and ionization potentials by using coupled cluster theory. It was suggested that the main features of the dynamics can be explained with the reduced two-dimensional (2D) space defined by the N–H and H–Cl collinear coordinates [5]. It is clear that the non-adiabatic effect between the ground and excited electronic states of neutral NH_3Cl plays a crucial role in the early-time dynamics of the dissociation process.

Ronen et al. [5] applied the quantum wave-packet propagation method to the adiabatic 2D potential energy surfaces (PESs) to uncover more details of the non-adiabatic effect on the early-time (<14 fs) dynamics of the

dissociation; the special emphasis of their study was the inclusion of the second-order non-adiabatic coupling term between the ground and the excited electronic states of neutral NH_3Cl. The early-time dynamics of NH_3Cl has been previously studied by Ronen et al. [5] and was investigated again in the present study with three new goals in mind that should provide additional insights into the details of the ultra-fast dynamics of this molecule.

The first goal was to provide a diabatic picture that provides increased physical intuition about the early-time non-adiabatic dissociation dynamics. For this purpose, a simple three-step diabatization procedure was developed that can generate the diabatic PESs and the coupling term between them by using just two adiabatic PESs; this procedure is described in Sect. 2.3. Although the theoretical approach with adiabatic representation of Ronen et al. [5] is more rigorous than the approach with diabatic representation of the present study, the computational demands of the kinetic coupling terms required by their approach are not always practical for large polyatomic systems. However, all of the methods generating diabatic representation are neither rigorous nor straightforward, especially for polyatomic systems, and trials to find easier diabatization methods and tests of their reliability are still an important part of research in the field of theoretical molecular dynamics. We found that the results obtained with our diabatic representation are in good agreement with the previous results of Ronen et al. [5], but that they also have the advantage that the diabatic PESs provide a clearer physical description of the early-time dynamics.

Our other two goals were to determine the effects on the early-time dynamics of deuterium (D) substitution (H_2NDCl) and of changes in the vibration level of the initial anion, NH_3Cl^-. These two goals might contribute to possible methods for the control of the ultra-fast dynamics, as investigated in many recent studies including our own [6].

2 Details of the computations

2.1 Wave-packet propagation

The time-dependent Schrödinger equation in the 2D space of the present study is defined as [7],

$$i\hbar\frac{\partial}{\partial t}\chi(q_1,q_2,t) = \hat{H}\chi(q_1,q_2,t), \tag{1}$$

$$\hat{H} = \hat{T}(q_1,q_2) + V(q_1,q_2), \tag{2}$$

where χ is the wave-packet (the nuclear wave function) and $\hat{H}$ is the Hamiltonian describing the system. The kinetic operator ($\hat{T}$) for an AB + C → A + BC type reaction can be written in terms of the internal coordinates q_1 and q_2, which are the internal distances of AB and BC, respectively [8].

$$\hat{T}(q_1,q_2) = -\frac{1}{2m_{AB}}\frac{\partial^2}{\partial^2 q_1} - \frac{1}{2m_{BC}}\frac{\partial^2}{\partial^2 q_2} - \frac{\cos\theta}{2m_B}\frac{\partial^2}{\partial q_1 \partial q_2}, \tag{3}$$

$m_{AB} = (M_AM_B)/(M_A + M_B)$ and $m_{BC} = (M_BM_C)/(M_B + M_C)$ are defined in terms of M_A, M_B, and M_C, which are the masses of NH_2, H, and Cl, respectively. The angle θ is fixed at 180°, which corresponds to a collinear reaction.

When only two electronic states are involved, as in the dissociation dynamics of NH_3Cl, the potential energy $V(q_1, q_2)$ can be represented by the following two-dimensional matrix composed of diabatic potential energies because we are using diabatic representations [9] of electronic states.

$$V^{Dia}(q_1,q_2) = \begin{pmatrix} V_{1,Dia} & V_{12,Dia} \\ V_{12,Dia} & V_{2,Dia} \end{pmatrix} \tag{4}$$

The diagonal components, $V_{1,Dia}$ and $V_{2,Dia}$, define the diabatic PESs of the two electronic states, and the off-diagonal term, $V_{12,Dia}$, is the diabatic coupling (potential coupling) between the two diabatic electronic states.

The time-propagation of a quantum mechanical wave-packet is treated by solving the above time-dependent Schrödinger equation by using either the split operator [10] or the Chebyshev's [11] method implemented in the Wavepacket program [12], as discussed below.

2.2 Vibration wave-packets of the anion, NH_3Cl^-

The previous study [5] examined the dynamics only for initial wave-packets corresponding to the ground vibration level of the anion NH_3Cl^-. In order to study the effects of varying the initial vibration levels of the anion, the first requirement is the generation of wave-packets for different vibration levels.

Weiser et al. [13] studied the stationary nuclear structure and vibrational properties of NH_3Cl^- and NH_3Cl by using the MP2/Aug-cc-pVTZ method. The geometry and vibration properties obtained in our calculations with the B3LYP/Aug-cc-pVTZ method are very similar to those of Weiser et al. [13], as shown elsewhere.[1]

[1] Bond lengths and angles calculated by the B3LYP(MP2) method are R_{NH} = 101.3(101.0) pm, ∠HNH = 107.2°(107.0°) for NH_3 (in C_{3V}), and R_{NH2} = 101.6(101.2) pm, R_{NH4} = 103.0(102.8) pm, R_{ClH4} = 239.8(229.0) pm, $\angle H_2NH_3$ = 105.5°(105.2°), $\angle H_2NH_4$ = 104.9°(104.6°), $\angle ClH_4N$ = 168.4°(171.4°) for NH_3Cl^- (in C_S). The harmonic frequencies of (in cm^{-1}) of NH_3 are ω_1 = 3,469(3,534), ω_2 = 1,025(1,027), ω_3 = 3,588(3,665), ω_4 = 1,664(1,669), and those of NH_3Cl^- are ω_1 = 3,488(3,555), ω_2 = 3,270(3,317), ω_3 = 1,655(1,656), ω_4 = 1,173(1,175), ω_5 = 330(365), ω_6 = 140(168), ω_7 = 3,550(3,629), ω_8 = 1,690(1,699), ω_9 = 247(285). The MP2 results are from Ref. [13].

We constructed a two-dimensional (2D) potential energy surface for NH_3Cl^- by using the B3LYP/Aug-cc-pVTZ method, implemented in the Gaussian 03 suite of programs [14]. The 2D space is that used in a previous study [5] and consists of 2,744 grid points corresponding to 56 and 49 values of R_{N-H} and R_{H-Cl}, respectively. R_{N-H} (the N–H distance between the N atom and the H atom connected to the Cl atom, as shown in Fig. 1a) varies from 0.25 to 3.00 Å with 0.05 Å spacing, and R_{H-Cl} varies from 0.70 to 3.10 Å with the same spacing. The other geometric parameters are frozen at the values of the equilibrium molecular structure of NH_3Cl^- (see footnote 1). This 2D surface for the anion is the gray surface in Fig. 1b. The two adiabatic 2D PESs of neutral NH_3Cl obtained by Ronen et al. [5] are also shown in Fig. 1b in red and blue for the ground and excited states, respectively.

The vibration wave-packets of the anion in this 2D space were generated by solving the Schrodinger equation, Eqs. (1) and (2), with Chebyshev's imaginary-time-propagator method [11] implemented in the Wavepacket package [12]. The eigenvalues of some low-lying vibration states in this 2D space are given and compared with other theoretical values and some available experimental values [13, 15] in Table 1. The vibration in the (0,1) mode corresponds to the stretch of the weakly bound intermolecular H_2NH–Cl bond, whereas that of the (1,0) mode is the N–H stretch of the hydrogen connecting the nitrogen and chlorine atoms. The harmonic frequencies (see footnote 1) calculated with

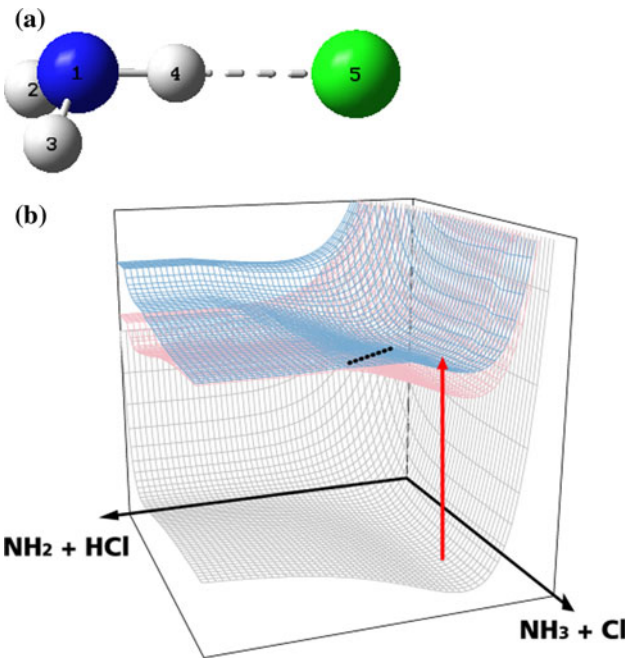

Fig. 1 **a** The equilibrium geometry of NH_3Cl^-, and **b** the adiabatic PESs of NH_3Cl^- (ground state: *gray*) and NH_3Cl (ground state: *red*, excited state: *blue*) with arbitrary energy spacing between the anion and neutral PESs

Table 1 The vibration eigenvalues (in cm^{-1}) of NH_3Cl^- and NH_2DCl^-

Method	Vibration	Value
B3LYP/Aug-cc-pVTZ[a]	ν (0,1)	134[b]
	ν (1,0)	3,139[b]
MP2/Aug-cc-pVTZ[c]	ν (0,1)	158[b]
	ν (1,0)	3,118[b]
Exp.	ν (1,0)	3,140 ± 10[c]
		3,121 ± 1[d]
Chebyshev's imaginary-time-propagator method (NH_3Cl^-)[a]	ν (0,1)	141
	ν (0,2)	277
	ν (1,0)	3,070
	ν (1,1)	3,223
	ν (1,2)	3,371
	ν (2,0)	5,917
	ν (2,1)	6,087
	ν (2,2)	6,250
Chebyshev's imaginary-time-propagator method (NH_2DCl^-)[b]	ν (0,1)	137
	ν (0,2)	269
	ν (1,0)	2,279
	ν (1,1)	2,423
	ν (1,2)	2,563
	ν (2,0)	4,445
	ν (2,1)	4,600
	ν (2,2)	4,749

[a] This study

[b] Result of multiplying the harmonic frequency (see footnote 1) obtained with the B3LYP(MP2) method by 0.96 (0.94)

[c] Ref. [13]

[d] Ref. [15]

the B3LYP(MP2) method are multiplied by a scale factor of 0.96 (0.94) to partially include the anharmonic effect, and the resulting values are in satisfactory agreement with the corresponding experimental results [13, 15]. The eigenvalues of the (0,1) and (1,0) modes, which were determined with Chebyshev's method and are shown in the middle of Table 1, are also very close to the experimental values, in spite of the fact that our values were obtained with the restricted 2D space. The results for the isotope-substituted system, H_2NDCl, given in the lower part of Table 1, show the changes in the eigenvalues due to the isotope effect; that is, the values of the (0,1) and (1,0) modes decrease from 141 and 3,070 to 137 and 2,279 cm^{-1}, respectively, as expected.

The vibration wave-packets of some low-lying levels are shown as the black contours in Fig. 2. The wave-packets were calculated with the PES of the anion, yet they are drawn on the contours of the diabatic PESs of the $V_{1,Dia}$ (red, dotted) and $V_{2,Dia}$ (blue, dotted) states of neutral H_2NHCl for convenience, particularly for the discussion of

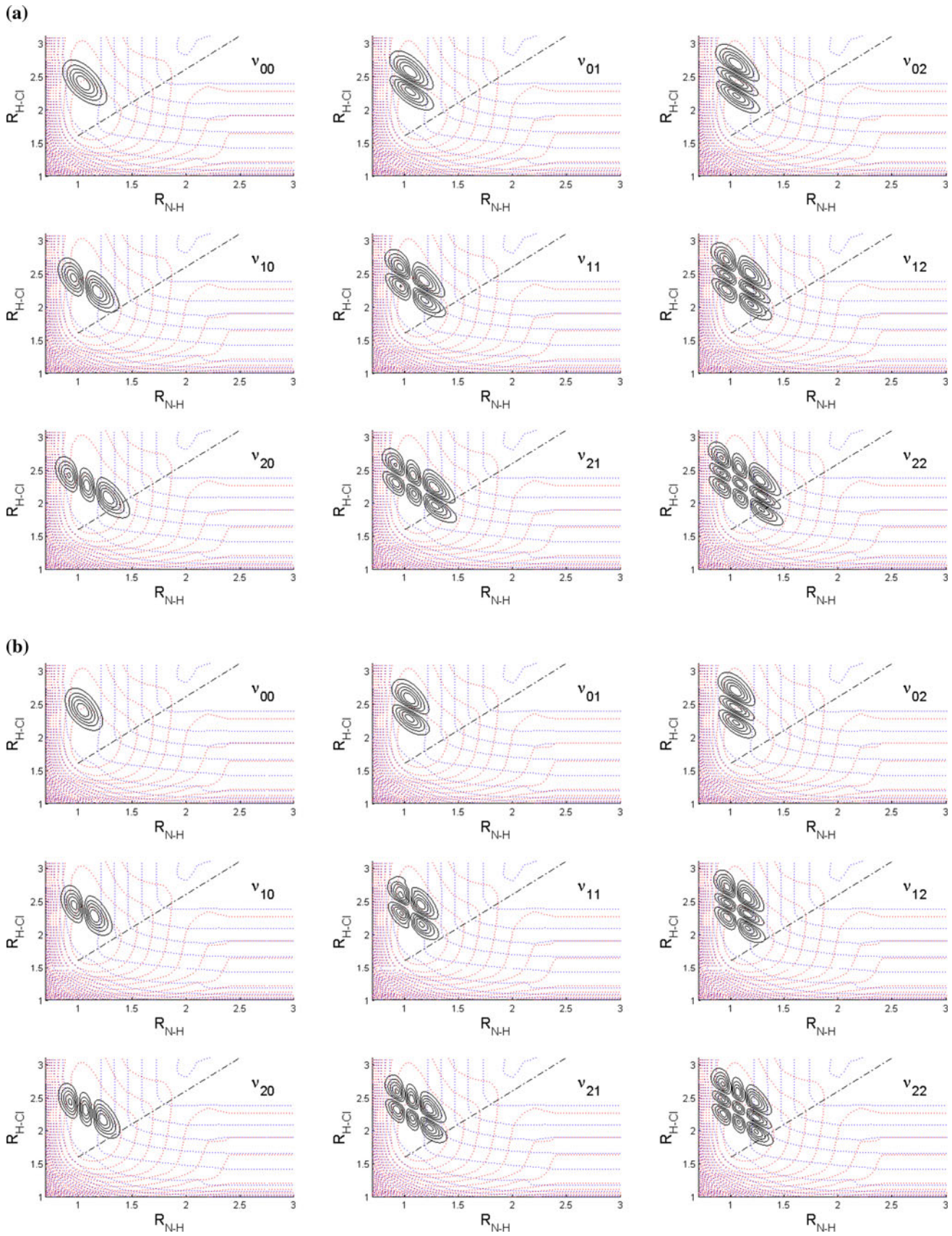

Fig. 2 Contour representations of the wave-packets of **a** H_2NHCl^- and **b** H_2NDCl^-

the dynamics of this system in Sect. 3. The crossing-lines between the two diabatic electronic states are also shown in each figure. Although the overall characteristics of the vibration wave-packets of the deuterium-substituted system (H_2NDCl^-) are almost the same as those of H_2NHCl^-, the wave-packets become a little more compact as a result of the isotope substitution. When a wave-packet of the anion is vertically excited to the $V_{2,\mathrm{Dia}}$ PES of neutral NH_3Cl by the photo-electron detachment, small changes in the spatial distribution of the wave-packet and its relation to the crossing-line can affect the details of the dissociation dynamics; investigating this effect was one of the goals of the current study, and it is discussed further in Sect. 3.

2.3 Diabatization of the adiabatic PESs of neutral NH_3Cl

In this subsection, we describe our three-step procedure for generating diabatic PESs and the coupling term between them from the adiabatic PESs of NH_3Cl.

Step 1: Initial diabatization is carried out by using the simple formula suggested by Gonzalez and coworkers; [16] this formula is applicable because the two electronic states of neutral NH_3Cl come close to each other along an almost linear curve (for convenience, this line is referred to as the 'crossing-line' hereafter), as in the case studied by Gonzalez and coworkers. As mentioned by Ronen et al. [5], the crossing-line corresponds approximately to the points where the two bond lengths, $R_{\mathrm{N-H}}$ and $R_{\mathrm{Cl-H}}$, differ by 0.6 Å. The following equation of Gonzalez and coworkers [16] is used to determine the mixing angle τ in Step 1.

$$\tau = \frac{\pi}{4} + \frac{\pi}{4}\tan^{-1}(\Gamma D(q_1, q_2)) \tag{5}$$

D is the distance from the crossing-line to a target position (q_1, q_2), and Γ is an empirical parameter that is adjusted to obtain smooth diabatic PESs. A unitary transformation matrix U is defined for a selected Γ value as follows:

$$U = \begin{pmatrix} \cos\tau & -\sin\tau \\ \sin\tau & \cos\tau \end{pmatrix} \tag{6}$$

Then, the energies of the diabatic states (V_{Dia}) can be obtained from the energies of the adiabatic states (V_{Adia}) by using the unitary transform matrix:

$$V_{\mathrm{Dia}} = U^{+} V_{\mathrm{Adia}} U \tag{7}$$

The actual values of $V_{1,\mathrm{Adia}}$ and $V_{2,\mathrm{Adia}}$ were obtained from the previous study [5].

To obtain a qualitative assessment of the diabatic PESs resulting from Step 1, one-dimensional (1D) cuts of the 2D PESs along the line perpendicular to the crossing-line are shown in Fig. 3a for a few selected values of Γ. (Note that only a crossing-point on the crossing-line is shown in this 1D cut.) For regions of the PESs sufficiently far from the crossing-line, the arc-tangent function, Eq. (5), does not depend strongly on the value of Γ and converges to a similar value. Therefore, far from the crossing-line, the resulting diabatic PESs are satisfactory for any reasonable value of Γ. For regions of the PESs near the crossing-line, however, the situation becomes more complicated.

Figure 3a shows that the diabatization with $\Gamma = 10$ (the blue dotted lines) results in a too narrow range of diabatization and, as a result, noticeable swellings (wrinkles) are present in the 2D PES near the crossing-line; the sudden curvature of the blue dotted lines of the 1D cut in Fig. 3a implies the presence of wrinkles. On the other hand, the diabatizations with Γ larger than 30 (the red dotted lines) result in diabatic PESs with the non-adiabatic range too wide. According to our several trials, the optimal Γ value in this case seems to be around 20 (the black dotted lines). However, the 2D diabatic PESs with $\Gamma = 20$ still have many small wrinkles scattered around the crossing-line. We have carried out some preliminary time-propagations with initial test wave-packets, which resulted in obviously questionable behavior around such wrinkles. In spite of our many attempts to make the range of the non-adiabatic region reasonable and to remove such small irregular wrinkles, diabatizations relying solely on simple functions such as Eq. (5) do not seem satisfactory.

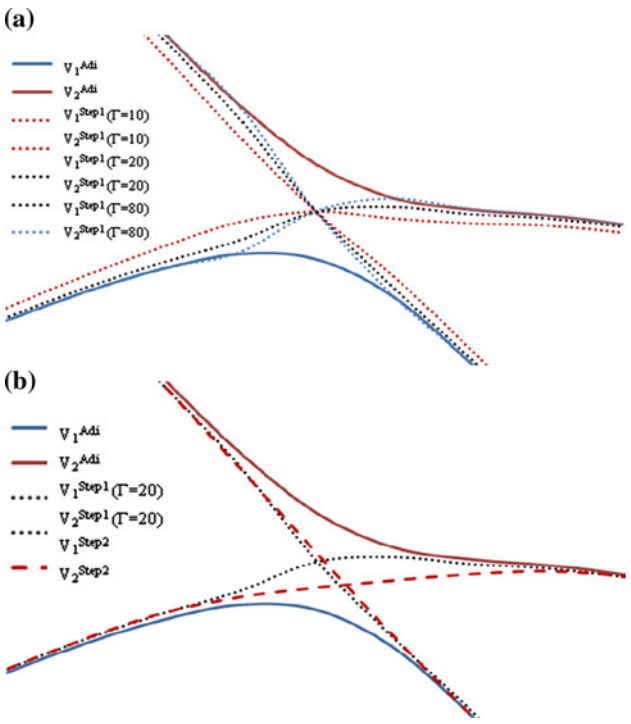

Fig. 3 **a** One-dimensional (1D) cuts of the diabatic PESs generated with various values of Γ with Step 1, and **b** a comparison of 1D cuts of the PESs obtained with Steps 1 and 2

Step 2: Refinement of the initial diabatic PESs is carried out by using a very simple criterion, that is, smoothness, which is the most basic requirement of diabatic PESs [9]. To improve the smoothness of the PESs generated with $\Gamma = 20$ in Step 1, the numeric values of $V_{1,\mathrm{Dia}}$ and $V_{2,\mathrm{Dia}}$ of the small wrinkles near the crossing-line are discarded and generated again with a linear interpolation method. Typical results of such a procedure are shown in Fig. 3b: the curves of the 1D cut of the diabatic PESs obtained with Step 1 are represented by black dotted lines, and the curves corresponding to the PESs obtained with linear interpolation in Step 2 are shown as red dashed lines. Note that the slight swelling near the crossing-point in the initial 1D cut (black dotted line) has been removed by the linear interpolation. It is also noticeable that the crossing-point between the two diabatic PESs has moved slightly outward as a result of this refinement, as can be seen in Fig. 3b. The choice of the swelling areas (i.e., the range of the wrinkle areas) and the refinement of those areas with linear interpolation are determined heuristically rather than rigorously, and some arbitrariness is present. However, we found that this procedure is not much difficult or ambiguous and that the final results of the wave-packet propagation discussed in Sect. 3 are not strongly dependent on the details of the fitting, at least in the case of this system. However, it should be mentioned that to apply linear interpolation directly to the original adiabatic PESs, without passing through Step 1, seems too arbitrary.

Step 3: The diabatic coupling term between the diabatic PESs is generated as follows. Once we have determined the energies of the diabatic PESs, i.e., $V_{1,\mathrm{Dia}}$ and $V_{2,\mathrm{Dia}}$ in Eq. (4), by performing Steps 1 and 2, a new mixing angle τ' is defined by the following equation.

$$\tau' = \sin^{-1}\sqrt{\frac{1}{2}\left(1 - \frac{V_{1,\mathrm{Dia}} - V_{2,\mathrm{Dia}}}{V_{1,\mathrm{Adi}} - V_{2,\mathrm{Adi}}}\right)} \tag{8}$$

Then, the value of the potential coupling term, $V_{12,\mathrm{Dia}}$ in Eq. (4), is calculated as follows.

$$V_{12,\mathrm{Dia}} = (V_{2,\mathrm{Adi}} - V_{1,\mathrm{Adi}}) \sin\tau' \cos\tau' \tag{9}$$

The values of $V_{12,\mathrm{Dia}}$ at all grid points of the 2D space are calculated with the above procedure. The two diabatic PESs ($V_{1,\mathrm{Dia}}$ and $V_{2,\mathrm{Dia}}$) and the potential coupling ($V_{12,\mathrm{Dia}}$) between them are shown in Fig. 4.

2.4 Assessment of the diabatic PESs

In spite of the arbitrariness in the above diabatization procedure, this method is computationally simple, and understanding of the dynamics obtained through wave-packet propagation can be simpler with the resulting diabatic PESs. In order to assess the reliability of our diabatic

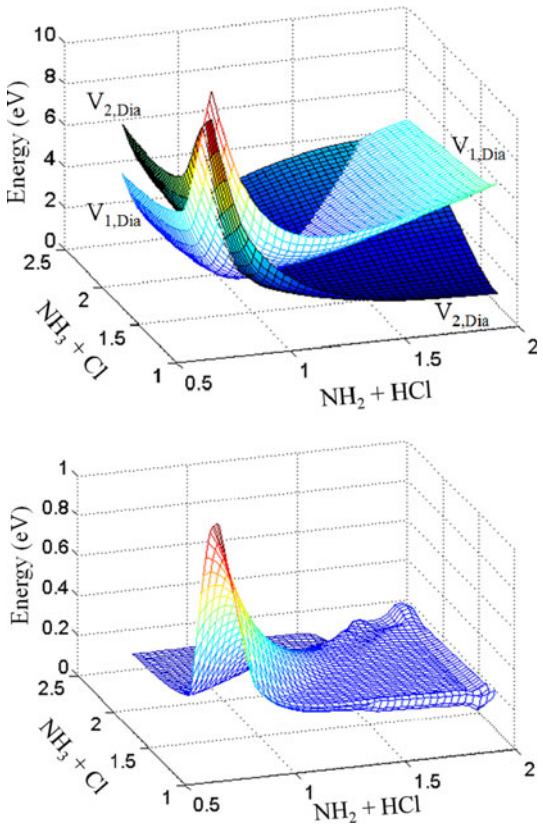

Fig. 4 Two diabatic PESs (*upper*) of NH_3Cl and the potential coupling between them (*lower*)

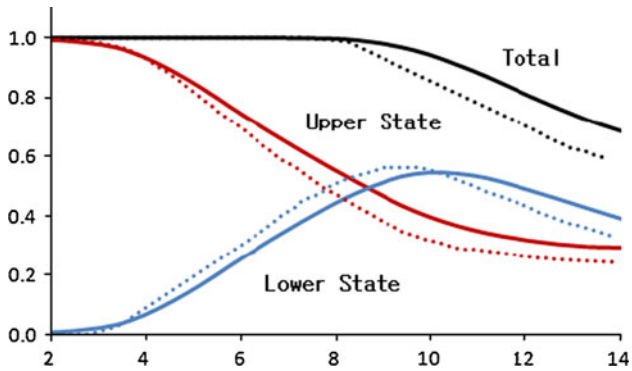

Fig. 5 The change in population with the time of propagation of the $v_{0,0}$ wave-packet of H_2NHCl^-. The *solid lines* are our results, and the *dotted lines* are the results of Ronen et al. [5]

PESs, the results obtained with our diabatic approach (the solid lines in Fig. 5) are compared with the results of the study of Ronen et al. (the dotted lines in Fig. 5) [5]. For a direct comparison, the populations of diabatic states obtained in our calculations are projected onto the populations of adiabatic states by using the method included in the Wavepacket program [12]. In addition to the basic difference between their non-adiabatic approach and our diabatic approach, there is also a slight difference between

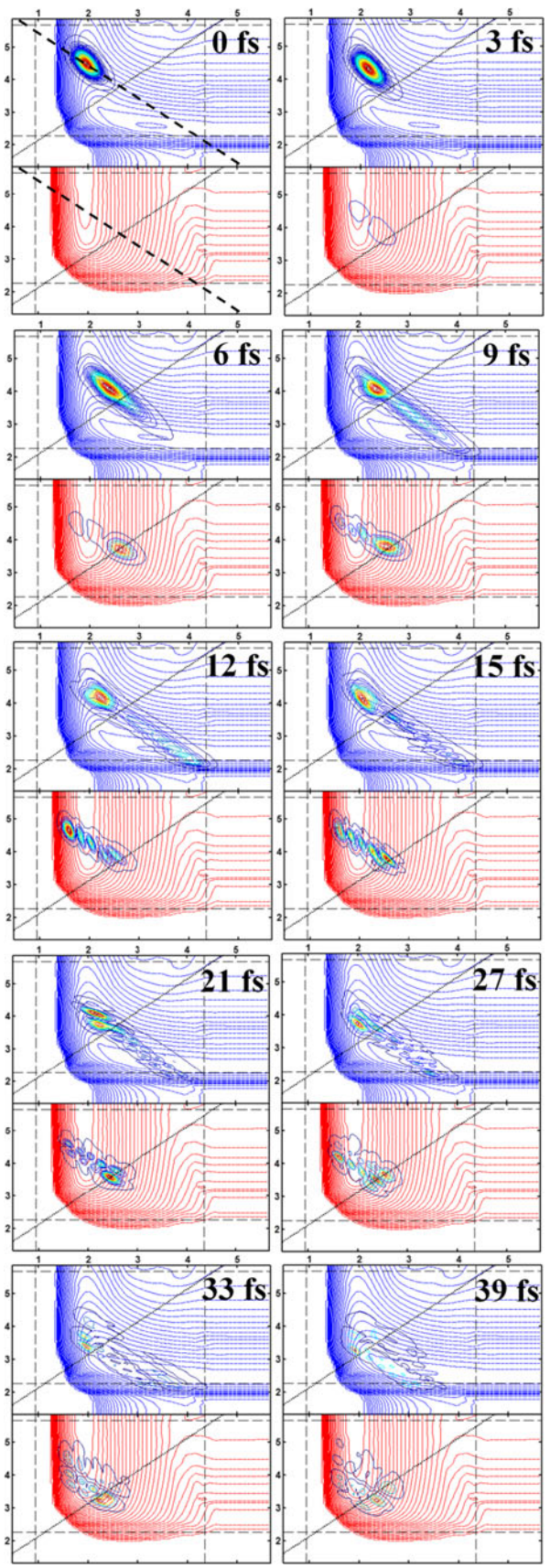

Fig. 6 Diabatic representations of the wave-packet dynamics after vertical excitation of $H_2NH\cdots Cl^-$ to the charge-transferred excited state, $H_2N^+H\cdots Cl^-$. The *upper* (*blue*) and *lower* (*red*) panels of each pair show the $V_{2,Dia}$ and $V_{1,Dia}$ PESs, respectively

the wave-packets. The initial wave-packet of Ronen et al. was created by projecting the harmonic ground-state vibrational function of the anion onto the N–H and H–Cl coordinates [5], whereas the v_{00} wave-packet generated in Sect. 2.2 was used in the present study, which means that intrinsic anharmonicity is included in our v_{00} wave-packet. Due to these small differences, our results do not match the previous results perfectly. The comparison in Fig. 5 does however show that the early-time dynamics are quite successfully described by our diabatic approach, not only qualitatively but also quantitatively, implying that the diabatic PESs and potential coupling generated in the present study are sufficiently reliable.

3 Results and discussion

3.1 Diabatic picture of the early-time dynamics

One of the main advantages of investigating dynamics with diabatic PESs rather than adiabatic PESs is the clearer physical picture. Some snapshots of the propagation of the initial wave-packet corresponding to the v_{00} vibration level of the anion are shown in Fig. 6. The adiabatic representation corresponding to the first three pairs in Fig. 6 is Fig. 3 of the previous paper [5]. The horizontal and the vertical axes in the figure indicate the dissociation channels toward HCl and Cl, respectively. In each snapshot, the upper (blue) and lower (red) panels represent the $V_{2,Dia}$ and $V_{1,Dia}$ PESs, respectively, and the wave-packet for each state is represented by a contour of the same color as the state. A negative imaginary potential (NIP) [17] of a power-function form was placed at the horizontal and vertical dashed lines in the figures to absorb the wave-packet corresponding to the dissociating portion. The main features of the early-time dissociation dynamics of H_2NHCl can be explained more easily with the 1D cut shown in Fig. 7, where the horizontal coordinate corresponds to the diagonal dashed line in the first pair (at 0 fs) of Fig. 6. The details of the ultra-fast features of the bidirectional proton–electron transfer [1] in the early-time dynamics can be described as follows.

The position of the initially excited wave-packet in the Franck–Condon region is indicated by **I** in Fig. 7, and the main characteristics of the initially excited state at **I** correspond to H_2NH^+–Cl^-, as mentioned in previous studies [2, 5]. According to the main concept behind the

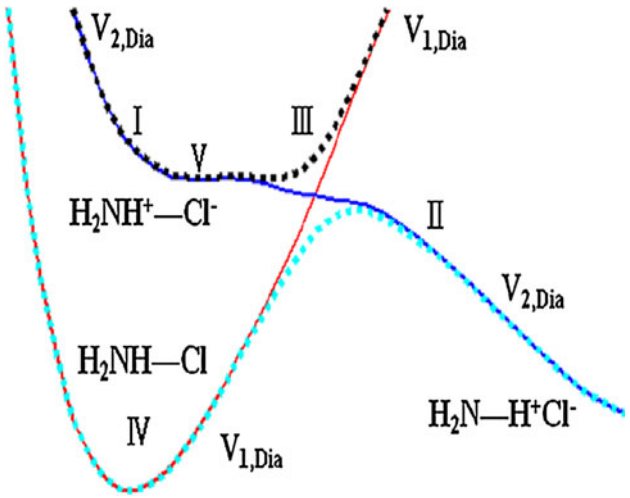

Fig. 7 The changes in the characteristics of the electronic states during the early-time dynamics of H_2NHCl. The *horizontal* coordinate corresponds to the *dashed line* in the first pair (at 0 fs) of Fig. 6. The FC position of the initially excited wave-packet is at **I**

diabatization, the characteristics of an electronic state are conserved along the diabatic PES, and the nuclear wave-packet propagating along the diabatic $V_{2,Dia}$ PES maintains the characteristics of the initial electronic state at position **I**. As a result, the wave-packet propagated to position **II** corresponds to H_2N–H^+Cl^-, because the change in the molecular geometry upon this propagation corresponds to an increase in the N–H distance and a simultaneous decrease in the H–Cl distance. This propagation can be described as the movement of the proton (H^+) without adjustment of the electronic distribution, that is, a *diabatic proton transfer*. At position **II,** the wave-packet propagates further along the same direction while the excess electron charge on Cl^- moves to H^+, and dissociation to the $H_2N + HCl$ limit eventually occurs. Thus, this dynamics can be characterized as diabatic proton transfer followed by electron adjustment.

As the wave-packet originating from position **I** propagates and bifurcates (the first bifurcation) at the crossing-point between the two PESs, one part propagates in the right-hand direction to position **III** along $V_{1,Dia}$. The steep increase in $V_{1,Dia}$ means that this part is actually trapped near the crossing position, as can be deduced from the almost fixed position of the center of the wave-packet on $V_{1,Dia}$ (red panels) at 6 and 9 fs in Fig. 6. The electronic characteristics of position **IV** correspond to H_2NH–Cl, as mentioned in previous studies [2, 5], and because position **III** is connected to position **IV** by $V_{1,Dia}$, the electronic character of the wave-packet leached (and trapped) at position **III** corresponds to H_2N–HCl, according to the change in molecular geometry described above. This **I** → **III** process can be described as the approach of a proton to Cl^- and the simultaneous adjustment of the excess electronic charge at Cl^- toward the approaching proton; this dynamics can thus be characterized as the attraction of an electron to the approaching proton. This direction of propagation, however, is not dissociative, and the wave-packet has to change its direction of propagation due to the steep increase in $V_{1,Dia}$ and then propagates backward. The returning wave-packet can bifurcate again (the second bifurcation) at the crossing-point toward positions **IV** or **V**.

The wave-packet leached at position **IV** now has the characteristics of H_2NH–Cl, and the movement **III** → **IV** corresponds to the simultaneous movement of electron along the proton, that is, the usual adiabatic dynamics. The important and interesting point clarified by this diabatic picture is that the dynamics from the charge-transferred excited state, H_2NH^+–Cl^-, to the ground H_2NH–Cl state do not consist of a simple electron transfer from the anionic part to the cationic part, even in this simple single-bonded system. The electron transfer is mediated (or stimulated) by the movement of the proton. The other part of the second bifurcation propagates along the PES of $V_{2,Dia}$ and arrives at position **V**, but the **III** → **V** proportion is negligibly small, as expected from the slopes of $V_{1,Dia}$ and $V_{2,Dia}$. Meanwhile, the center of the original wave-packet on $V_{2,Dia}$ (blue panels) has moved to position **V**, as shown by the snapshots at 9, 12, and 15 fs in Fig. 6, because position **V** corresponds to the stationary structure of $V_{2,Dia}$, as shown in Fig. 7.

According to Ronen et al. [5], if the initial wave-packet produced by the electron photo-detachment with low energy (~4 eV) is placed not in the charge-transferred excited state but in the ground electronic state of NH_3Cl, the wave-packet is trapped in the stationary structure of the ground electronic state, and no dissociation to the $H_2NH + Cl$ or $H_2N + HCl$ limit occurs. However, the wave-packet at position **IV** that results from the movement **III** → **IV** could have much larger kinetic energy than the wave-packet initially prepared by the low-energy photon, and so can propagate further to the $H_2NH + Cl$ limit. However, according to our simulations, almost no part of the wave-packet with this high kinetic energy propagates to the $H_2NH + Cl$ limit, mainly due to the perpendicular nature of the kinetic energy with respect to the dissociation path. The snapshots at 21, 27, 33, and 39 fs in Fig. 6 show that no part of the wave-packet on $V_{1,Dia}$ (red panels) propagates toward the $H_2NH + Cl$ limit (left-upper side). Instead, the wave-packet on $V_{1,Dia}$ smears out into the $H_2N + HCl$ region (right-lower side) via a kind of tunneling effect, that is, an adiabatic tunneling of an H atom.

According to our calculations with the G3 method [18], the energy of the $H_2N + HCl$ limit is 13 kJ/mol higher than that of the $H_2NH + Cl$ limit.[2] Moreover, the barrier to the $H_2NH + Cl$ limit (left-upper side) is much lower than that to the $H_2N + HCl$ limit. Therefore, the perpendicular nature (with respect to the reaction coordinate toward the $H_2NH + Cl$ limit) of the kinetic energy of the wave-packet at position IV seems to be the main reason for the adiabatic tunneling of an H atom toward the $H_2N + HCl$ limit. This result could be an artifact caused by the restrictions of the 2D space used in this study, but it is worth to note that no Cl product was observed in previous experiments [2, 3].

To summarize this diabatic picture of the dissociation dynamics of the charge-transferred excited state of H_2NHCl, the path toward the $H_2N + HCl$ limit includes two processes: single-step dynamics featuring '*diabatic proton transfer followed by electron adjustment*,' and two-step dynamics consisting of the formation of the ground electronic state of H_2NH–Cl via '*electron transfer from the other direction mediated (stimulated) by proton movement*' followed by adiabatic H atom tunneling to H_2N–HCl. It may be an additional detailed aspect of the wide range of proton-coupled electron-transfer (PCET) phenomena [1].

3.2 Effects of varying the vibration level of NH_3Cl^-

The changes in the total populations (population dynamics) with the propagation time are shown in Fig. 8; the population dynamics commencing with different vibration levels of the anion are represented by different colors (black, red, and blue for the 0, 1, and 2 levels, respectively, of the internal N–H stretch mode) and different types of lines (solid, dotted, and dashed for the 0, 1, and 2 levels, respectively, of the H_2NH–Cl stretch mode). The decrease in the total population below 1.0 is caused by the absorption of the wave-packet by the NIP placed at the horizontal dashed lines in Fig. 6; it corresponds to the formation of the HCl product.

Note the shift in the early-dissociation time; the early-dissociation time is estimated here as the time when the total population decreases below 0.9. The value 0.9 was chosen partially because the lines of different types but with the same color cross each other around that value. When the vibration level of the internal H_2N–H stretch mode (lines with different colors) is excited from $0 \rightarrow 1$ and $1 \rightarrow 2$, the early-dissociation time is shortened by approximately 3 and 1 fs, respectively. On the other hand, the excitations in the vibration level of the H_2NH–Cl stretch mode (different types of lines) turn out to have

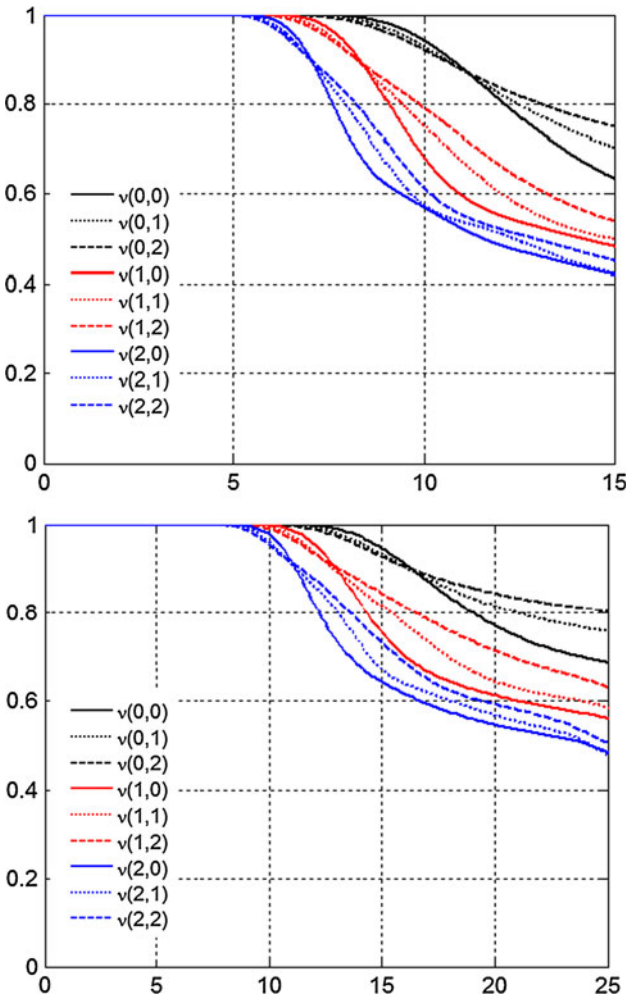

Fig. 8 The changes in the total populations of H_2NHCl (*upper*) and H_2NDCl (*lower*), depending on the initial vibration level, with the wave-packet propagation time (in fs)

negligible effects on the early-dissociation time. There are some marginal effects, that is, the higher the level of the H_2NH–Cl stretch mode, the slower the dissociation dynamics beyond the early-dissociation time.

Although the changes in the populations after 15 fs were generated in our study, we refrain from further detailed discussions of these changes because the effects of the other seven internal vibration modes of NH_3Cl were not included in the dynamics studied here. If the dimensionality of the system were increased, the timescale of the dissociation dynamics would be shortened still further.

The initial purpose of our study of different initial vibration levels was to determine the changes in the branching ratio of the two dissociation paths toward the $H_2NH + Cl$ and $H_2N + HCl$ limits. According to our study, however, almost no part of the wave-packet reaching position IV of Fig. 7 dissociates to the $H_2NH + Cl$ limit, as described above in Sect. 3.1. As a result, only the $H_2N + HCl$ dissociation products are observed in our

[2] G3(0 K) energies are −459.990959(Cl), −56.507020(NH_3), −460.654664(HCl), and −55.848193 (NH_2) Hartrees.

simulation, regardless of the initial vibration levels. The extension to higher dimensionality seems to be indispensable for future theoretical studies aiming at finding a method of controlling the branching ratio of the two channels.

3.3 Effects of isotope substitution, H_2NDCl

The effects of isotope substitution on the dissociation dynamics were tested for H_2NDCl by using the same diabatic PESs and coupling term of NH_3Cl as shown in Fig. 4. The completely substituted system, D_2NDCl, might be more relevant to actual experiments, but H_2NDCl was investigated in this study because the difference between the isotope effects of H_2NDCl and ND_3Cl is small, as is expected from the marginal change in mass M_A indicated by Eq. (3). The overall shapes of the vibration wave-packets of H_2NDCl are almost the same as those of H_2NHCl, but their spatial extents in Fig. 3b are a little more compact than those of NH_3Cl^- in Fig. 3a. The vibration energies of H_2NDCl are noticeably smaller than those of NH_3Cl^-, as shown in Table 1. The smaller eigenvalues implies a smaller intrinsic kinetic energy of the wave-packets, and much longer timescales (slower kinetics) are anticipated.

The qualitative features of the population dynamics of H_2NDCl, shown in the lower panel of Fig. 8, are almost the same as those of H_2NHCl shown in the upper panel of Fig. 8. The dependence of the dynamics on the vibration levels of the initial wave-packet is also very similar to that in the case of H_2NHCl. The main difference is the timescale: the early-dissociation time is increased by a factor of approximately one and a half by the isotope substitution. This retardation of the dynamics is also reflected in the less steep slope of the decrease in the total population, even after the early-dissociation time.

4 Conclusion

A simple diabatization scheme, generating smooth diabatic PESs and the potential coupling term between them by using just two adiabatic PESs, is demonstrated and applied to the charge-transfer excited state of the NH_3Cl system. The results of our study are in good agreement with those of a previous study [5], which accounted for not only the first- but also the second-order non-adiabatic coupling terms, so future applications of the simple diabatization method to other systems are promising, at least for those systems that can be treated with a restricted two-dimensional space.

By using this diabatic picture in this present study, it was demonstrated that the dissociation toward the HCl product from the charge-transferred excited state, H_2NH^+–Cl^-, includes two different processes: the one-step dynamics of '*diabatic proton transfer followed by electron adjustment*,' and the two-step dynamics consisting of the formation of the ground electronic state of H_2NH–Cl by '*electron transfer from the other direction mediated (stimulated) by proton movement*' followed by adiabatic H atom tunneling to H_2N–HCl.

In order to find a method of controlling the branching ratio of the dissociation paths toward the H_2N + HCl and H_2NH + Cl limits, we studied the effects of varying the vibration levels of the anion H_2NHCl^-, which is the precursor of the excited electronic state of neutral H_2NHCl arising from electron photo-detachment, on the early-time (<15 fs) dissociation dynamics. According to the present study, however, no product of the H_2NH + Cl limit is observed regardless of the initial vibration levels. The extension of this approach to higher dimensionality is highly desirable for future theoretical studies aiming at controlling the branching ratio of the two channels. A decrease of a few femtoseconds in the early-dissociation time is observed upon the activation of one quantum of the vibration level (of around 3,121–3,140 cm^{-1}) of the hydrogen vibration between the N and Cl atoms of H_2NHCl^-. On the other hand, the dynamics are slightly slowed by the excitation of the vibration level corresponding to the stretch of the weak intermolecular H_2NH–Cl bond, but the effects are negligible.

The effects of deuterium substitution of the active H atom, H_2NDCl^-, were also studied. Although the effects of varying the vibration levels on the early-time dynamics are almost unaltered by the isotope substitution, the timescale of the dynamics is slowed down by a factor of approximately one and a half.

We hope our current results will motivate further theoretical and experimental studies of the interesting NH_3Cl system, which is the first described case of a non-adiabatic chemical reaction triggered by electron photo-detachment, as advocated by an earlier study [5].

Acknowledgments This study was supported by grants (2011-0003830, 2011-0001213) of the National Research Foundation of Korea. This work was also supported by R&D Program through the National Fusion Research Institute (NFRI) of Korea funded by the Government funds (No. 1345165741). Computational resources were partially supported by KISTI.

References

1. Hammes-Schiffer S, Stuchebrukhov A (2010) Chem Rev 110:6939
2. Markovich G, Cheshnovsky O, Kaldor U (1993) J Chem Phys 99:6201
3. Markovich G, Cheshnovsky O (1994) J Phys Chem 98:3550

4. Kaldor U (1994) Z Phys D 31:279
5. Ronen S, Nachtigallova D, Schmidt B, Jungwirth P (2004) Phys Rev Lett 93:048301
6. An H, Baeck KK (2011) J Phys Chem A 115:13309
7. Tannor D (2007) Introduction to quantum mechanics: a time-dependent perspective. University Science Book, Sausalito
8. Schinke R (1993) Photodissociation dynamics. Cambridge University Press, Cambridge
9. Baer M (2006) Beyond born-oppenheimer: electronic nonadiabatic coupling terms and conical intersections. Wiley, London
10. Feit MD, Fleck JA Jr, Steiger A (1982) J Comput Phys 47:412
11. Kosloff R, Tal-Ezer H (1986) Chem Phys Lett 127:223
12. Schmidt B, Lorenz U (2009) WavePacket4.7: a program package for quantum-mechanical wavepacket propagation and time-dependent spectroscopy. Available via http://wavepacket.sourceforge.net
13. Weiser P, Wild D, Wolynec P, Bieske E (2000) J Phys Chem A 104:2562
14. Pople JA et al. (2004) Gaussian 03, revision E.01. Gaussian, Inc., Wallingford
15. Tschurl M, Boesl U (2008) Chem Phys Lett 456:150
16. Rozgonyi T, Gonzalez L (2008) J Phys Chem A 112:5573
17. Kosloff R, Kosloff D (1986) J Comput Phys 63:363
18. Curtiss LA, Raghavachari K, Redfern PC, Rassolov V, Pople JA (1998) J Chem Phys 109:7764